

## Research Article

# Comprehensive reliability and performance estimation of multi-state sequential system through general and copula repair techniques

Ibrahim Yusuf <sup>1,\*</sup>, Kabiru Garba Ibrahim <sup>2</sup>, Hamisu Ismail Ayagi <sup>3</sup>

1. Department of Mathematical Science, Bayero University, Kano, Nigeria
2. Department of Mathematics, Federal University, Dutse, Nigeria
3. Yusuf Maitama Sule University

 <https://doi.org/10.71720/joie.2025.1184950>

**Received:** 23 September 2024  
**Revised:** 01 December 2024  
**Accepted:** 13 December 2024

### Keywords:

Availability;  
Serial;  
Reliability;  
System;  
Sensitivity

### Abstract

The purpose of this work is to look into some of the dependability aspects of measuring the effectiveness of a four-subsystem serial system. Subsystem 1 has one unit in series with other subsystems, subsystem 2 has three units in parallel, subsystem 3 has three units in parallel, and subsystem 4 has three units in parallel. In a series configuration, both subsystems are connected partially and completely failing the system is a possibility. The partial failure mode is thought to have left the system in a degraded state, whereas the total failure mode causes the system to stop functioning. Failures are assumed to follow an exponential distribution, whereas repair is assumed to follow one of the general or Gumbel-Hougaard family copulas. The system is investigated using an extra variable and the Laplace transform. Profit analysis was derived by utilizing dependability parameters such as availability, reliability, and Mean Time to Failure (MTTF). The system has been investigated throughout the project. The computed results were displayed in a graph, and the value of the analysis was conveyed in the conclusion section. The analysis of tables and figures highlights the effectiveness and applicability of both the copula approach and the general repair framework. Notably, the copula-based repair method exhibits superior reliability, availability, and profitability compared to the general repair framework. Furthermore, the findings aid pump decision-makers in anticipating future advances in pump performance, ensuring the safe and reliable operation of water pumps. It can also be employed in additional applications that require greater head and flow pumps.

### Citation:

usuf, I., Ibrahim, K. G., & Ayagi, H. I. (2025). Comprehensive Reliability and Performance Estimation of Multi-State Sequential System through General and Copula Repair Techniques. *Journal of Optimization in Industrial Engineering*, 18(1), 91-113. <https://doi.org/10.71720/JOIE.2025.1184950>



### \* Corresponding Author:

**Ibrahim Yusuf**

Department of Mathematical Science, Bayero University, Kano, Nigeria  
E-Mail: [iyusuf.mth@buk.edu.ng](mailto:iyusuf.mth@buk.edu.ng)



This article is an open access article distributed under the terms and conditions of the Creative Commons Attribution (CC BY-NC) license (<https://creativecommons.org/licenses/by/4.0/>).

## 1. Introduction

In the realm of engineering, manufacturing, production and industrial operations, ensuring the reliability and performance of critical systems is paramount. Multi-state sequential systems (MSS) are particularly significant as they encompass a variety of operational states beyond simple binary conditions of functionality or failure. These systems, including centrifugal pumps, play crucial roles in numerous applications, ranging from water supply and wastewater treatment to chemical processing and energy production. The complexity of these systems necessitates advanced methodologies for accurate reliability and performance estimation. Centrifugal pumps, in particular, are integral components in many industrial processes due to their ability to handle a wide range of fluids and operating conditions. Their performance impacts not only the efficiency but also the safety and sustainability of the systems they serve. For instance, in water supply systems, the reliability of centrifugal pumps is crucial for ensuring a continuous and safe water supply. In chemical processing, any failure in the pumps can lead to significant production losses and safety hazards. Therefore, precise reliability and performance estimation methods are essential for maintaining and improving the operational integrity of these systems. Traditional reliability and performance assessment methods often fall short in addressing the nuanced behavior of MSS, particularly when accounting for the diverse operational states and the interdependencies between components. These conventional approaches typically simplify the system into binary states of functioning or failure, which do not capture the intermediate states of partial functionality that are common in real-world applications. Moreover, they often assume independence between components, overlooking the critical interdependencies that can significantly impact overall system performance.

Numerous studies in the field of reliability engineering have demonstrated that effective performance analysis can prevent disasters and save both money and time. Here are a few, Yemane and Colledani (2019) introduced a performance assessment framework to evaluate the efficiency of uncertain manufacturing systems with unreliable machines. Their approach focuses on assessing how uncertainties impact manufacturing processes and system reliability. Zhao et al. (2021) explored and optimized the economic performance of a cold standby system that is vulnerable to shocks and imperfect repairs. They proposed geometric process models to quantify both the lifetime and repair time of the system, offering a comprehensive analysis of its economic performance under various conditions. Xie et al. (2021) studied methods to enhance the performance of safety instrumented systems (SIS) in mitigating incidents and reducing cascading failures. They emphasized the importance of considering the reliability and durability of SIS in preventing cascading failures. Using Monte Carlo simulations, they validated their method through iterative combinations within a reliability block diagram framework. Xie et al. (2019) built upon the work of Wang et al. (2018) by creating models to investigate the effects

of cascading failures in railway signaling systems. Their research aimed to determine the average frequency of critical failures in high- or continuous-demand mode systems that are prone to cascading failures, providing valuable insights into system reliability and failure prevention strategies.

Abubakar and Singh (2019) used a copula linguistic technique to examine the performance of an industrial system. Poonia (2021) conducted an in-depth analysis of the performance measures of a computer network system, which is structured as a series-parallel system incorporating four integrated subsystems. The system under study comprises two load balancers (LB), five web servers (WB), and three database replica servers (DBRS). Each of these components plays a critical role in ensuring the seamless operation and reliability of the network by employing the k-out-of-n redundancy approach to model the subsystems' reliability. By integrating these subsystems into a cohesive series-parallel architecture, key performance metrics such as system reliability, availability, and mean time to failure (MTTF) are developed and analyzed numerically.

Singh et al. (2020) conducted a comprehensive study focusing on the reliability and performance measures of a complex system, which is organized into two subsystems arranged in a series configuration and supported by a switching device. The system's design is intended to ensure high reliability and performance through the implementation of specific redundancy policies for each subsystem. Subsystem-1 operates under a 2-out-of-5: G policy, while subsystem-2, on the other hand, is governed by a 1-out-of-2: G policy. They evaluated key metrics such as system reliability, availability, mean time to failure (MTTF), and mean time to repair (MTTR). Their analysis provided insights into how the redundancy policies of the subsystems and the functionality of the switching device contribute to the overall system performance.

Singh et al. (2021) delve into the performance modeling and assessment of a complex, repairable system composed of two subsystems arranged in series. Each subsystem contains multiple identical units, operating under the (k-out-of-n: G) scheme, where the system functions successfully if at least k out of n units are operational. Key performance metrics evaluated in the study include system reliability, availability, mean time to failure (MTTF), and mean time to repair (MTTR). The findings provide insights into how the (k-out-of-n: G) redundancy scheme influences these metrics, demonstrating how different configurations of n units and k thresholds impact the robustness and efficiency of the subsystems.

Singh and Poonia (2022) undertake a comprehensive investigation into the reliability and performance measures of a complex system featuring two subsystems arranged in a series configuration, presenting a valuable opportunity for addressing specific design challenges. In this system architecture, Subsystem-1 comprises n units operating under the k-out-of-n: G policy, while Subsystem-2 consists of m units functioning under the r-out-of-m: G policy. Various performance metrics, including system reliability, availability, mean time to failure (MTTF), and mean time to repair (MTTR). Yusuf et al. (2020) created models to

examine the reliability and performance of a multi-computer system comprising three subsystems arranged in a series configuration, employing copula repair policies.

The primary objectives of this research are three. The first is to comprehensively evaluate the centrifugal system, focusing on critical parameters such as availability and reliability. Key performance metrics, including mean time to failure (MTTF), sensitivity analysis of MTTF, and profit, form integral components of this assessment. A secondary objective involves modeling the intricate interdependencies among system components that influence the efficiency and dependability of centrifugal systems. This is achieved using the copula methodology, which provides a robust framework for capturing these complex relationships. Finally, the study aims to develop a practical framework by integrating insights from the copula-based analysis. This framework is designed to optimize the design and performance of centrifugal systems, enhancing their operational efficiency. By bridging theoretical insights with practical implementation, this research significantly advances the system's overall effectiveness, reliability, resilience, robustness, and performance.

## **2. Related Works and Contributions of the Current Research**

Several researchers have studied manufacturing, industrial, and production systems under various operating constraints and situations, providing insights into the reliability and performance of these systems. Qazizada and Pivarciova (2018) focused on the reliability of parallel and serial centrifugal pumps used for dewatering. They conducted a reliability study on centrifugal pumps connected in parallel and serial configurations at different frequencies of rotation (DFR) and flow rates to understand their behaviors. Their research aimed to identify how these configurations affect the pumps' operational stability and efficiency under varying conditions, providing valuable data for optimizing pump arrangements in industrial dewatering applications.

Mortazavi et al. (2018) employed a combined alpha-factor model and a capacity flow model to calculate the Mean Time Between Failures (MTBF) of a 2-out-of-3 repairable redundant centrifugal water pumping system. Their study accounted for common cause and cascade failures, integrating fuzzy failure rates and repair rates into their calculations. By considering these complex failure mechanisms and uncertainties, Mortazavi et al. provided a more comprehensive and realistic assessment of the system's reliability. Their findings offer significant insights for improving the maintenance strategies and design of redundant pumping systems, ensuring higher reliability and reduced downtime in critical water supply operations.

The failure analysis of centrifugal pumps was studied by Selvakumar and Natarajan (2015). They collected and analyzed data on the lifespan of pump components and the frequency of problems occurring within these pumps. Their survey recorded detailed information on the life expectancy of various pump components and identified common issues that frequently arise. By analyzing this data, Selvakumar and Natarajan were able to pinpoint the

most vulnerable parts of centrifugal pumps and the typical causes of failure. This information is crucial for improving maintenance practices, extending the service life of pumps, and enhancing overall reliability in industrial applications. Jiang et al. (2019) conducted a comprehensive review of centrifugal pumps based on experimental data. Their study aimed to identify the significant geometrical parameters that impact pump head degradation, particularly in single-stage centrifugal pumps operating in two-phase flow situations. By examining a range of geometrical factors, Jiang et al. sought to understand how these variables influence pump performance and contribute to head degradation. Their findings provide valuable insights into optimizing pump design and configuration to minimize performance losses and ensure efficient operation under challenging two-phase flow conditions. This research is instrumental in guiding the development of more robust and reliable centrifugal pumps for various industrial applications.

Hawash et al. (2015) conducted an in-depth investigation into the use of inducers to enhance the reliability of centrifugal pumps. They evaluated the impact of inducers on pump performance through a series of hydraulic tests aimed at determining the optimal hydraulic performance both before and after the implementation of inducers. Their research focused on identifying improvements in pump efficiency, pressure head, and overall operational stability, providing valuable insights into how inducers can be utilized to extend the lifespan and reliability of centrifugal pumps in various applications.

Jilani and Razali (2017) focused on the performance characteristics of centrifugal pumps designed for household use. They developed and validated a test rig to monitor and analyze the performance of these pumps under different operating conditions. Their study aimed to assess key performance metrics such as flow rate, head, efficiency, and power consumption. By systematically testing and validating the pumps, Jilani and Razali provided detailed performance profiles that can guide the selection and optimization of centrifugal pumps for domestic water supply systems, ensuring reliable and efficient operation in household environments.

Ahmed et al. (2016) investigate the use of inlet guided vanes to enhance the efficiency of centrifugal water pumps. They examine the effects of various pre-whirling angles on the pump's efficiency and head, as well as the performance curves generated under different operating conditions. Their study aims to identify optimal pre-whirling angles that can maximize pump performance, leading to more energy-efficient and effective pump operation.

Kumar et al. (2018) assessed mechanical problems associated with centrifugal pumps in Eastern Uttar Pradesh, India. Their evaluation provides a comprehensive overview of the common issues faced by pumps in this region, contributing to a better understanding of maintenance needs and potential areas for improvement in pump design and operation.

Sayed (2020) introduced a classification model for centrifugal pump failure detection based on neural networks, using copula linguistics. The study presents the

development of an artificial neural network (ANN) model for fault classification and detection, integrated with vibration-based condition monitoring. This approach involves constructing an ANN model capable of recognizing faults in a centrifugal pumping system, with the model being tested and refined using two simulated faults. The study demonstrates the effectiveness of using neural networks for accurate fault detection, aiming to improve the reliability and maintenance of centrifugal pumps through advanced predictive techniques.

Bordeasu et al. (2024) present a novel formula designed to estimate pump efficiency, a critical factor for accurately determining power consumption, particularly in variable-frequency situations. The parameters of this formula are derived from experimental data collected from an existing pumping system. This innovative approach provides a more precise method for calculating pump efficiency, which is vital for optimizing energy usage and performance in various operational scenarios.

Cheng et al. (2022) conducted an in-depth examination of the transient hydraulic performance of a small centrifugal pump by measuring its external performance during the startup process under both power frequency and frequency conversion modes. To analyze the transient behavior of the pump during these startup modes, they employed three dimensionless parameters: the flow coefficient, the head coefficient, and the speed coefficient. These parameters allowed them to identify and compare the similarities and differences in the pump's performance under the two startup conditions. By focusing on these aspects, Cheng et al. aimed to gain a better understanding of the pump's dynamic behavior, providing valuable insights for improving pump design and operation under varying frequency conditions.

Zhu et al. (2019) propose a comprehensive performance and reliability analysis of centrifugal pumps using maintenance data. In their analysis, they employ the least squares method to estimate the parameters of the Weibull distribution, a widely used statistical distribution in reliability engineering for modeling failure times. This method helps in accurately fitting the Weibull distribution to the observed maintenance data, providing valuable insights into the failure patterns and lifespan of the pumps. To enhance the robustness and accuracy of their analysis, Zhu et al. (2019) utilize Monte Carlo sampling techniques. This approach involves generating a large number of simulated data points based on the observed data, effectively expanding the sample size. By doing so, they can perform a more thorough examination of the data, which leads to a more reliable and precise assessment of the pumps' performance and reliability over time. The Monte Carlo simulations allow them to account for variability and uncertainty in the data, resulting in a more comprehensive and detailed analysis of the centrifugal pumps' operational characteristics and failure behavior.

Dehnavi et al. (2023) study how the speed ratio between the inducer and the impeller affects pump performance in both co-rotation and counter-rotation modes. They perform a comparative analysis between numerical simulations of the inducer and impeller and the corresponding experimental results to determine their flow fields. On the

other hand, Shukla and Agrawal (2024) developed computational fluid dynamic models to evaluate the performance of a radial flow centrifugal pump, focusing on optimizing the pump's operational efficiency under various operating conditions. Pagayona and Honra (2024) investigate the impact of different inlet and outlet impeller diameters and varying numbers of impeller blades on pump performance. Their study involves three main stages: pre-processing, which includes geometry creation, meshing, and study configuration; processing, which covers defining physics settings, selecting the solver type, and specifying boundary conditions; and post-processing, which focuses on interpreting the results obtained from the model creation and solution. In contrast, Yuan et al. (2023) examine the effects of pitch motion on the performance characteristics and unsteady flow mechanisms of a centrifugal pump.

The existing body of literature has extensively explored various aspects of the performance and reliability of centrifugal water pumping systems, highlighting improvements in system efficiency and operational effectiveness. While these studies have contributed significantly to our understanding of centrifugal pumps, there remains a notable gap specifically concerning copula-based approaches. This gap pertains to the comprehensive examination of reliability, durability, performance, and dependability within centrifugal water pumping systems using copula methodologies. To bridge this research gap, this paper focuses on a detailed modeling of performance and a thorough assessment of reliability for a centrifugal water pumping system composed of four interconnected subsystems. The system under study is structured as follows: Subsystem 1: Its role is crucial as it serves as the initial point of control and regulation within the system. Subsystem 2: These parallel valves work together to manage the flow and pressure within the system, enhancing its efficiency and operational flexibility. Subsystem 3: In this subsystem, three centrifugal pump units are arranged in parallel. This parallel configuration is intended to increase the system's capacity and reliability by distributing the load among multiple pumps. Subsystem 4: Similar to Subsystem 2, this subsystem features three units in parallel. The air valves are essential for regulating airflow and pressure, contributing to the overall stability and performance of the system. By addressing the copula-based examination of these interconnected subsystems, this paper aims to provide a comprehensive understanding of how copula methodologies can enhance the modeling of performance and the assessment of reliability in centrifugal water pumping systems. This approach is expected to reveal insights into the complex interactions and dependencies between subsystems, thereby offering a more robust analysis of the system's overall reliability, durability, and performance. The study's findings will contribute to filling the existing research gap by applying copula-based methods to a detailed and practical examination of centrifugal water pumping systems, ultimately leading to improved strategies for system management and optimization.

The novelty of this study lies in its investigation of the dependability aspects of a four-subsystem serial centrifugal water pumping system, with a specific focus on:

1. Configuration of Subsystems: The unique setup includes various subsystems in series and parallel arrangements, with partial and total failure modes considered. This hybrid configuration analysis is less commonly addressed in existing studies.
2. Failure and Repair Models: The study utilizes exponential distributions for failures and introduces general or Gumbel-Hougaard family copulas for modeling repairs. This combination of probabilistic models provides a novel approach to understanding system dependability.
3. Analytical Techniques: Employing the Laplace transform and an extra variable for the investigation adds a novel methodological aspect to the dependability analysis.
4. Comprehensive Dependability Parameters: The study derives profit analysis using dependability parameters such as availability, reliability, and Mean Time to Failure (MTTF), offering a holistic view of the system's performance.
5. Practical Implications: The findings provide valuable insights for pump decision-makers to anticipate future advancements in pump performance and ensure the safe and reliable operation of water pumps, with potential applications in systems requiring higher head and flow pumps.

### 3. Notations and Description of the System

#### 3.1 Notations

$q$  to denote the time variable

$R_0(q)$  to denote the likelihood that the system will remain in state  $S_0$

$R_k(e_i, q)$  to denote the likelihood that the system will remain in state  $S_k$ ,  $k = 1, 2, 3, \dots, 22$  and  $i = 1, 2, 3, 4$

$\beta_0(e_i)$  to denote rate of general repair

$h_0(e_i)$  to denote rate of copula repair

$v_i$  to denote rate of failure of units in subsystem  $i$

$\bar{R}(q)$ : to represent the Laplace transformation of the probability of a state transition  $h(\mathcal{G}_0)$

$R_i(e_1, q)$ : To represent the probability that a system is in state  $S_i$  for  $i=1, \dots, 22$ , the system is in repair and the elapsed repair time is  $(e_1, q)$ , where  $e_1$  is the repair variable and  $q$  is the time variable.

$J_p(q)$ : to represent profit expected during the time interval  $[0, q]$

$\kappa_1, \kappa_2$ : Revenue and service cost per unit time respectively.

$S_\phi(\varepsilon_1)$ : Notation function  $S_\phi(\varepsilon_1) = \beta_0(e_1) e^{-\int_0^{\varepsilon_1} \beta_0(e_1) de_1}$  with repair distribution function  $\phi(\varepsilon_1)$ .

$\bar{S}_\phi(s)$ : Laplace transforms of  $S_\phi(x)$ , i.e.,

$$\bar{S}_\phi(s) = \int_0^\infty e^{-s\varepsilon_1} \phi(\varepsilon_1) e^{-\int_0^{\varepsilon_1} \beta_0(e_1) de_1} dx$$

$h_0(e) = C_\theta(h_1(e), h_2(e))$ : The expression of joint probability (failed state  $S_i$  to good state  $S_0$ ) according to Gumbel-Hougaard family copula is given as:

$$c_\theta(u_1(\varepsilon), u_2(\varepsilon)) = \exp\left(\varepsilon^\theta + \left\{\log \phi(\varepsilon)^\theta\right\}^{\frac{1}{\theta}}\right),$$

$1 \leq \theta \leq \infty$ . Where

$$\mu_1 = \phi(\varepsilon), \text{ and } u_2 = e^\varepsilon$$

$S_0$ : Initial state, the subsystems, and the system are in perfect state. The system is up and running.

$S_1$ : Unit in subsystem 1 failed. The system is down.

$S_2$ : One of the units failed in subsystem 2, other water valves are working. The system is up and running in reduced capacity.

$S_3$ : One of the units failed in subsystem 3 has failed, other units are working. The system is up and running in reduced capacity.

$S_4$ : One of the units failed in subsystem 4 has failed, other units are working. The system is up and running in reduced capacity.

$S_5$ : Two of the units failed in subsystem 2 have failed, the remaining unit is working. The system is up and running in reduced capacity.

$S_6$ : Previously one of the units in subsystem 3 have failed, followed by failure of one of the units in subsystem 2. The system is up and running in reduced capacity.

$S_7$ : Previously one of the units in subsystem 4 have failed, followed by failure of one of the units in subsystem 2. The system is up and running in reduced capacity.

$S_8$ : All the three units in subsystem 2 have failed. The system is down.

$S_9$ : Previously one of the units in subsystem 2 have failed, followed by failure of one of the units in subsystem 4. The system is up and running in reduced capacity.

$S_{10}$ : Two of the units failed in subsystem 4 have failed, the remaining unit is working. The system is up and running in reduced capacity.

$S_{11}$ : Previously one of the units in subsystem 3 have failed, followed by failure of one of the units in subsystem 4. The system is up and running in reduced capacity.

$S_{12}$ : All the three units in subsystem 3 have failed. The system is down.

S<sub>13</sub>: Previously one of the units in subsystem 2 have failed, followed by failure of one of the units in subsystem 4. The system is up and running in reduced capacity.  
 S<sub>14</sub>: Previously one of the units in subsystem 4 have failed, followed by failure of one of the units in subsystem 4. The system is up and running in reduced capacity.  
 S<sub>15</sub>: Two of the units failed in subsystem 4 have failed, the remaining unit is working. The system is up and running in reduced capacity.  
 S<sub>16</sub>: All the three units in subsystem 4 have failed. The system is down.  
 S<sub>17</sub>: Two of the units failed in subsystem 3 have failed, the remaining unit is working and one of the units have failed in subsystem 2. The system is up and running in reduced capacity.  
 S<sub>18</sub>: Two of the units failed in subsystem 4 have failed, the remaining unit is working and one of the units has failed in

subsystem 2. The system is up and running in reduced capacity.  
 S<sub>19</sub>: Two of the units in subsystem 2 have failed, the remaining unit is working and one of the units has failed in subsystem 3. The system is up and running in reduced capacity.  
 S<sub>20</sub>: Two of the units in subsystem 4 have failed, the remaining unit is working and one of the units has failed in subsystem 3. The system is up and running in reduced capacity.  
 S<sub>21</sub>: Two of the units in subsystem 3 have failed, the remaining unit is working and one of the units has failed in subsystem 4. The system is up and running in reduced capacity.  
 S<sub>22</sub>: Two of the units in subsystem 2 have failed, the remaining unit is working and one of the units has failed in subsystem 4. The system is up and running in reduced capacity.

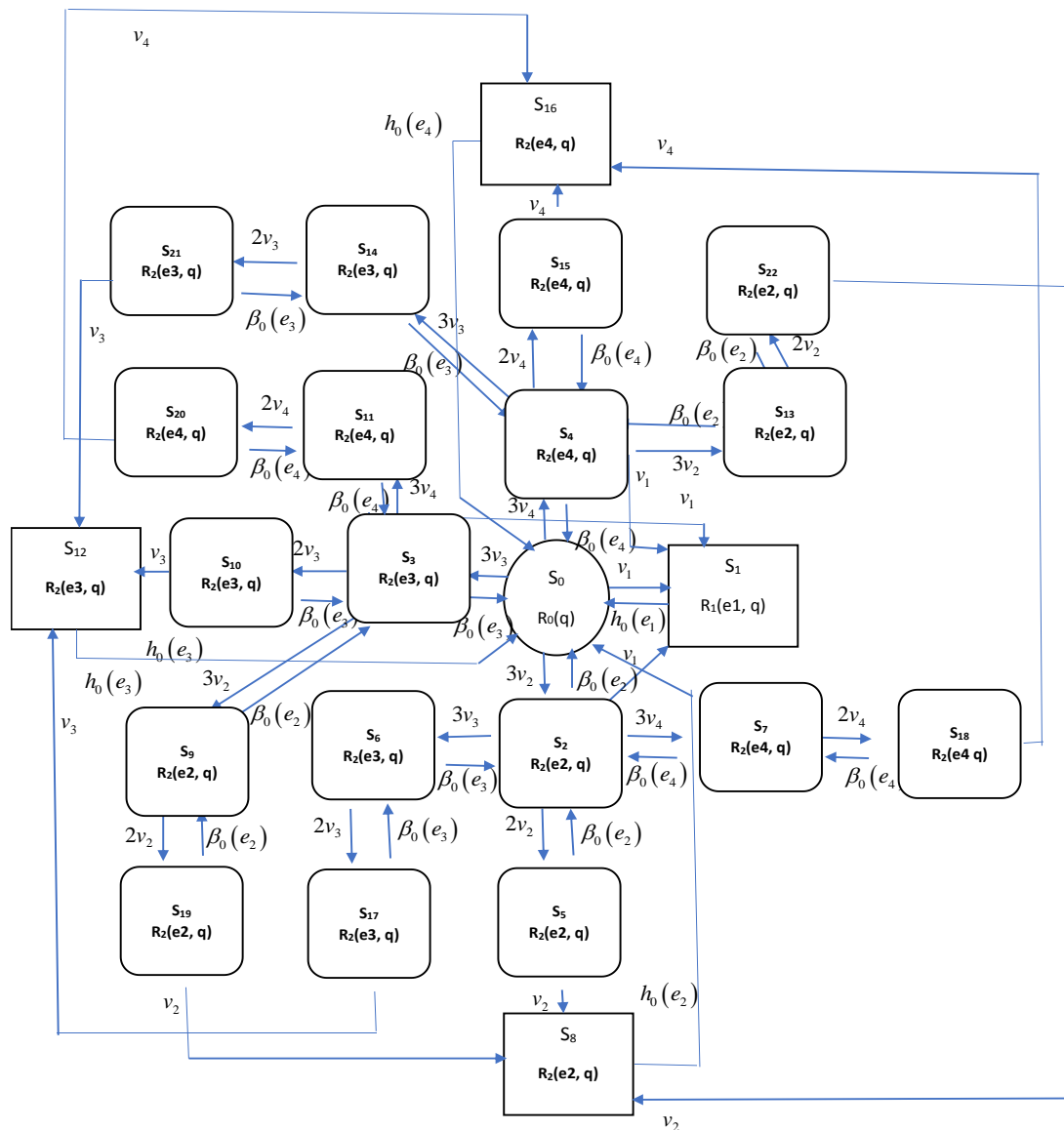


Fig. 1. Transition diagram of the system

#### 4. Methodology

Developing reliability and performance models for centrifugal systems using the transition diagram in Figure 1 and solving them with Laplace transformation and the supplementary variable technique is a multi-step process. Here's an overview:

1. Construct the Transition Diagram: Begin by creating a transition diagram (e.g., Figure 1) to represent the system's various states and transitions. Each state illustrates a specific condition or configuration, while transitions depict changes between these states. The diagram should incorporate factors affecting reliability, mean time to failure (MTTF), availability, and profit.
2. Define Variables and Parameters: Identify the key variables and parameters for your analysis, such as component failure rates, repair rates, transition probabilities, and system configurations.
3. Formulate Partial Differential Equations (PDEs): Use the transition diagram to derive transition rates between states, representing the likelihood of moving from one state to another. Express these rates as functions of the defined variables and parameters, forming PDEs that describe the rate of change of state probabilities over time.
4. Apply Laplace Transformation: Transform the PDEs into the frequency domain using the Laplace transformation. This simplifies the equations by converting time-dependent

derivatives into algebraic terms involving the Laplace variable.

5. Solve the Transformed Equations: Simplify and manipulate the transformed equations to determine state probabilities or other reliability and performance metrics. This step often requires algebraic rearrangement and solving for unknowns.
6. Perform Inverse Laplace Transformation: Convert the frequency-domain solutions back into the time domain using the inverse Laplace transformation. This step provides time-dependent insights into system behavior, such as state probabilities or performance metrics.
7. Analyze Results: Interpret the time-domain solutions to assess reliability, MTTF, availability, and profit. Evaluate these metrics to draw meaningful conclusions about the system's performance and effectiveness.

#### 5. Formulation of Reliability Models and their Solutions

To develop reliability models for system modeling and analysis, the supplementary variable technique and Laplace transforms were employed. A probabilistic approach facilitated the derivation of differential equations from the transition diagram. These differential equations were then solved using initial and boundary conditions to determine the steady-state probabilities. These probabilities form the foundation for the development of reliability models. The partial differential equations derived from Figure 1 are as follows:

$$\left(\frac{\delta}{\delta q} + v_1 + 3v_2 + 3v_3 + 3v_4\right)R_0(q) = \int_0^{\infty} \beta_0(e_2)R_2(e_2, q)de_2 + \int_0^{\infty} \beta_0(e_3)R_3(e_3, q)de_3 + \int_0^{\infty} \beta_0(e_4)R_4(e_4, q)de_4 + \int_0^{\infty} h_0(e_1)R_1(e_1, q)de_1 + \int_0^{\infty} h_0(e_2)R_8(e_2, q)de_2 + \int_0^{\infty} h_0(e_3)R_{12}(e_3, q)de_3 + \int_0^{\infty} h_0(e_4)R_{16}(e_4, q)de_4 \quad (1)$$

$$\left(\frac{\delta}{\delta q} + \frac{\delta}{\delta e_1} + h_0(e_1)\right)R_1(e_1, q) = 0 \quad (2)$$

$$\left(\frac{\delta}{\delta q} + \frac{\delta}{\delta e_2} + v_1 + 2v_2 + 3v_3 + 3v_4 + \beta_0(e_2)\right)R_2(e_2, q) = 0 \quad (3)$$

$$\left(\frac{\delta}{\delta q} + \frac{\delta}{\delta e_4} + v_1 + 3v_2 + 2v_3 + 3v_4 + \beta_0(e_4)\right)R_3(e_4, q) = 0 \quad (4)$$

$$\left(\frac{\delta}{\delta q} + \frac{\delta}{\delta e_4} + v_1 + 3v_2 + 3v_3 + 2v_4 + \beta_0(e_4)\right)R_4(e_4, q) = 0 \quad (5)$$

$$\left(\frac{\delta}{\delta q} + \frac{\delta}{\delta e_2} + v_2 + \beta_0(e_2)\right)R_5(e_2, q) = 0 \quad (6)$$

$$\left(\frac{\delta}{\delta q} + \frac{\delta}{\delta e_3} + 2v_3 + \beta_0(e_3)\right)R_6(e_3, q) = 0 \quad (7)$$

$$\left( \frac{\delta}{\delta q} + \frac{\delta}{\delta e_4} + 2v_4 + \beta_0(e_4) \right) R_7(e_4, q) = 0 \quad (8)$$

$$\left( \frac{\delta}{\delta q} + \frac{\delta}{\delta e_2} + h_0(e_2) \right) R_8(e_2, q) = 0 \quad (9)$$

$$\left( \frac{\delta}{\delta q} + \frac{\delta}{\delta e_2} + 2v_2 + \beta_0(e_2) \right) R_9(e_2, q) = 0 \quad (10)$$

$$\left( \frac{\delta}{\delta q} + \frac{\delta}{\delta e_2} + v_3 + \beta_0(e_3) \right) R_{10}(e_3, q) = 0 \quad (11)$$

$$\left( \frac{\delta}{\delta q} + \frac{\delta}{\delta e_4} + 2v_4 + \beta_0(e_4) \right) R_{11}(e_4, q) = 0 \quad (12)$$

$$\left( \frac{\delta}{\delta q} + \frac{\delta}{\delta e_3} + h_0(e_3) \right) R_{12}(e_3, q) = 0 \quad (13)$$

$$\left( \frac{\delta}{\delta q} + \frac{\delta}{\delta e_2} + 2v_2 + \beta_0(e_2) \right) R_{13}(e_2, q) = 0 \quad (14)$$

$$\left( \frac{\delta}{\delta q} + \frac{\delta}{\delta e_3} + 2v_3 + \beta_0(e_3) \right) R_{14}(e_3, q) = 0 \quad (15)$$

$$\left( \frac{\delta}{\delta q} + \frac{\delta}{\delta e_4} + v_4 + \beta_0(e_4) \right) R_{15}(e_4, q) = 0 \quad (16)$$

$$\left( \frac{\delta}{\delta q} + \frac{\delta}{\delta e_4} + h_0(e_4) \right) R_{16}(e_4, q) = 0 \quad (17)$$

$$\left( \frac{\delta}{\delta q} + \frac{\delta}{\delta e_3} + v_3 + \beta_0(e_3) \right) R_{17}(e_3, q) = 0 \quad (18)$$

$$\left( \frac{\delta}{\delta q} + \frac{\delta}{\delta e_4} + v_4 + \beta_0(e_4) \right) R_{18}(e_4, q) = 0 \quad (19)$$

$$\left( \frac{\delta}{\delta q} + \frac{\delta}{\delta e_2} + v_2 + \beta_0(e_2) \right) R_{19}(e_2, q) = 0 \quad (20)$$

$$\left( \frac{\delta}{\delta q} + \frac{\delta}{\delta e_4} + v_4 + \beta_0(e_4) \right) R_{20}(e_4, q) = 0 \quad (21)$$

$$\left( \frac{\delta}{\delta q} + \frac{\delta}{\delta e_3} + v_3 + \beta_0(e_3) \right) R_{21}(e_3, q) = 0 \quad (22)$$

$$\left( \frac{\delta}{\delta q} + \frac{\delta}{\delta e_3} + v_2 + \beta_0(e_3) \right) R_{22}(e_3, q) = 0 \quad (23)$$

## 6. Modeling Reliability Characteristics and Optimizing Performance

To conduct the numerical experiment, data for the system parameters is carefully assigned based on assumed or estimated values that are representative of the real-world

conditions of the centrifugal system. These parameters typically include failure rates, repair rates, transition probabilities, and other variables that influence the system's reliability and performance.

**6.1 Evaluation of availability when repair follows copula distribution**

If the repair follows Gumbel- Hougaard family copula distribution then, setting.

$$S_{\mu_0}(s) = \bar{S}_{\exp[e_1^\theta + \{\log \varphi(e_1)\}^\theta]^{1/\theta}}(s) = \frac{\exp[e_1^\theta + \{\log \varphi(e_1)\}^\theta]^{1/\theta}}{s + \exp[e_1^\theta + \{\log \varphi(e_1)\}^\theta]^{1/\theta}}$$

$$\bar{S}_\phi(s) = \frac{\phi}{s + \phi}, \text{ and taking the values of different}$$

parameters as  $\phi = \mu = x = 1$ , and using failure rates as  $v_1 = 0.011, v_2 = 0.012, v_3 = 0.013, v_4 = 0.014$  in equation (118) and inverting the Laplace to have

$$R_{up}(q) = \left\{ \begin{array}{l} -0.0005336e^{-1.01300q} + 0.004789e^{-2.73154q} - 0.015240e^{-1.21995q} - \\ 4.065562e^{-1.11560q} - 4.041333e^{-1.11444q} + 1.016132e^{-0.00975q} - \\ 0.000612e^{-1.01400q} - 0.001324e^{-1.02400q} - 0.001390e^{-1.02800q} - \\ 0.000457e^{-1.01200q} - 0.001362e^{-1.02600q} \end{array} \right\} \quad (120)$$

For availability examination, considering passage of time  $q \in [0, 20]$  to have Table 1 and Figure 2

Table 1  
 Time passage with the corresponding Availability for Copula repair

Time	0	2	4	6	8	10	12	14	16	18	20
Availability	1.0000	0.9944	0.9770	0.9583	0.9398	0.9216	0.9038	0.8868	0.8692	0.8524	0.8359

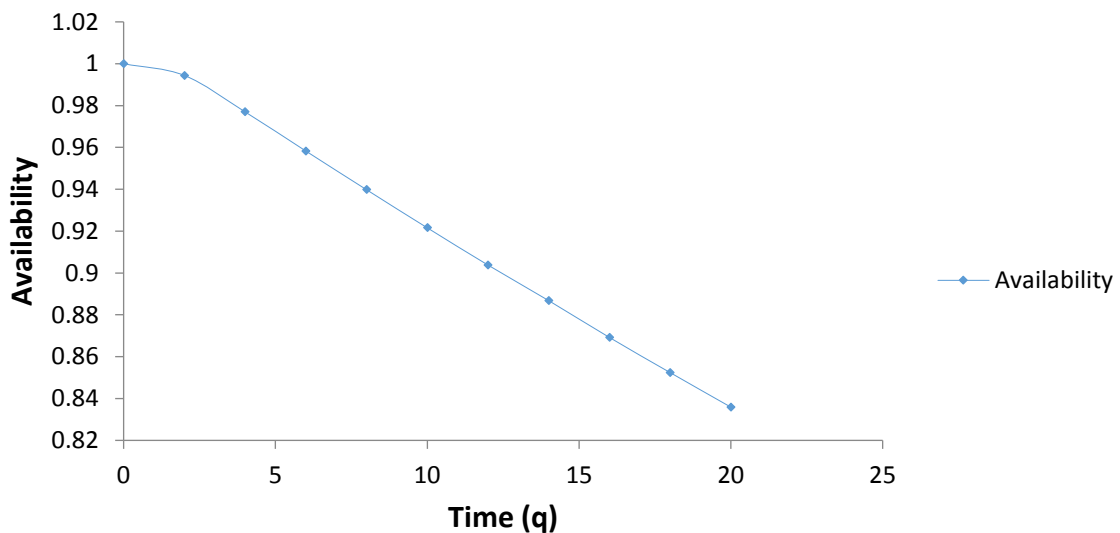


Fig. 2. Time passage with availability for Copula repair

**6.2 Evaluation of availability when repair follows general repair**

For availability, considering time  $q \in [0, 20]$  Table 2 and Figure 3 are constructed using equation (121)

$$R_{up}(q) = \left\{ \begin{array}{l} -0.000462e^{-1.01200q} - 0.00539e^{-1.01300q} - 0.000618e^{-1.01400q} - \\ 0.001402e^{-1.02800q} - 0.001374e^{-1.02600q} - 0.001336e^{-1.00400q} - \\ 0.013911e^{-1.22191q} - 3.467964e^{-1.11560q} - 3.450628e^{-1.11444q} + \\ 1.019643e^{-1.02104q} \end{array} \right\} \quad (121)$$

Table2  
 Effect of Time on System Availability via General Repair Policy

Time	0	2	4	6	8	10	12	14	16	18	20
Availability	1.0000	0.9756	0.9371	0.8986	0.8616	0.8261	0.7920	0.7594	0.7281	0.6981	0.6693

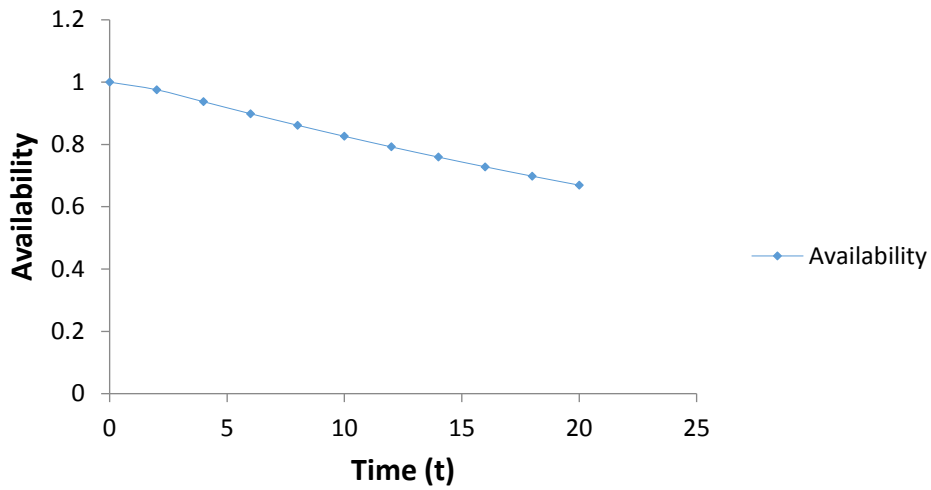


Fig. 3. Time passage with availability for General repair

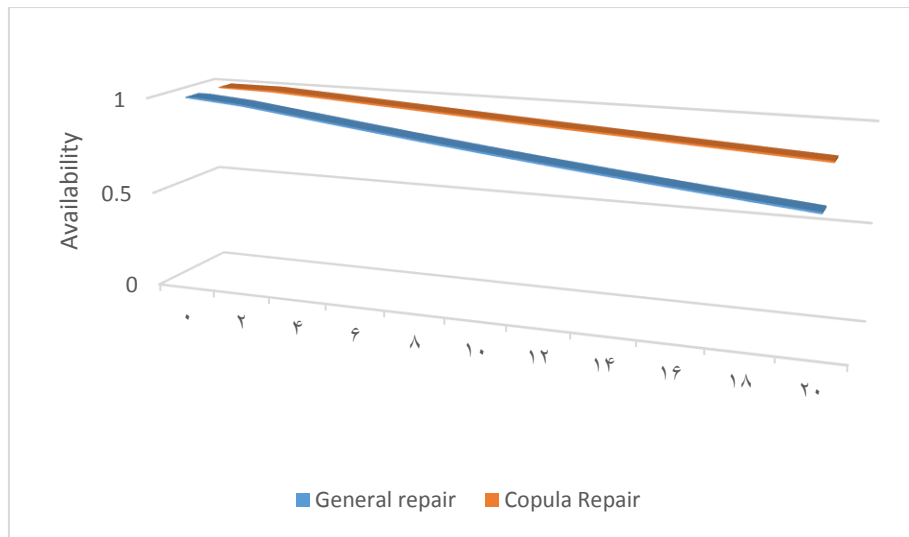


Fig. 4. Time passage with availability with respect to Copula and General repair

6.3 Evaluation of reliability

Following the similar procedure in 5.1 and 5.2, all repairs assigned to zero, and inverting the Laplace, the reliability model of the system is

$$R_E(q) = \left\{ \begin{array}{l} 0.031500e^{-0.02800q} + 0.011089e^{-0.04100q} + 0.029823e^{-0.02600q} + \\ 0.028038e^{-0.02400q} + 0.009529e^{-0.01300q} + 0.008051e^{-0.01200q} + \\ 8.118032e^{-0.12800q} + 3e^{-0.11400q} + 3e^{-0.11500q} + 3e^{-0.11600q} \end{array} \right\} \quad (122)$$

Table 3  
 Time passage with the corresponding reliability

Time	0	2	4	6	8	10	12	14	16	18	20
Reliability	1.0000	0.9790	0.9241	0.8508	0.7694	0.6867	0.6068	0.5323	0.4644	0.4036	0.3500

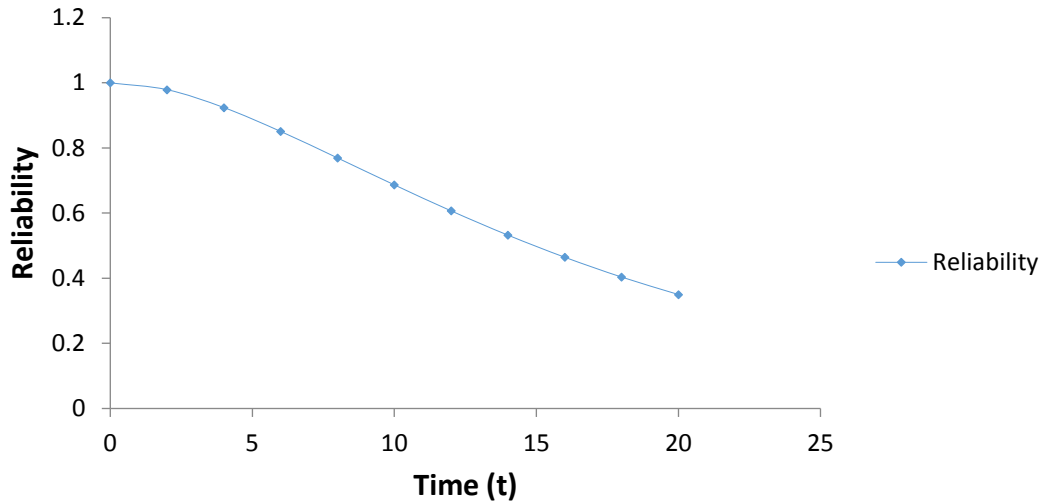


Fig. 5. Effect of Time on System Reliability

6.4 Mean time to failure analysis

Taking all repairs to zero in Equation (118) and the limit when  $s$  approaches zero, the formula for MTTF

$$MTTF = \lim_{s \rightarrow 0} \bar{R}_{up}(s)$$

can be written as:

$$= \frac{1}{v_1 + 3v_2 + 3v_3 + 3v_4} \left\{ 1 + \frac{3v_2}{v_1 + 2v_2 + 3v_3 + 3v_4} + \frac{3v_3}{v_1 + 3v_2 + 2v_3 + 3v_4} + \frac{3v_4}{v_1 + 3v_2 + 3v_3 + 2v_4} + 15v_2 + 15v_3 + 15v_4 + \frac{54v_2v_4 + 18v_2v_3 + 36v_3v_4}{v_1 + 3v_2 + 3v_3 + 2v_4} \right\} \quad (123)$$

Fixing  $v_1 = 0.011$ ,  $v_2 = 0.012$ ,  $v_3 = 0.013$ ,  $v_4 = 0.014$  and varying the failure rate under investigation as 0.01, 0.02, 0.03, 0.04, 0.05, 0.06, 0.07, 0.08, 0.09

respectively, the variance of MTTF with respect to failure rates as shown in Table 4 and Figure 6 can be obtained in the above equation.

Table 4  
 Calculated MTTF for Different Failure Rates

Failure rate	$MTTF v_1$	$MTTF v_2$	$MTTF v_3$	$MTTF v_4$
0.001	23.0366	25.8272	26.4806	27.0641
0.002	22.7546	25.1515	25.7608	26.3084
0.003	22.4789	24.5277	25.0976	25.6139
0.004	22.2094	23.9495	24.4843	24.9730
0.005	21.9458	23.4118	23.9149	24.3793
0.006	21.6879	22.9102	23.3876	23.8274
0.007	21.4357	22.4410	22.8894	23.3127
0.008	21.1888	22.0008	22.4254	22.8312
0.009	20.9472	21.5868	21.9897	22.3796

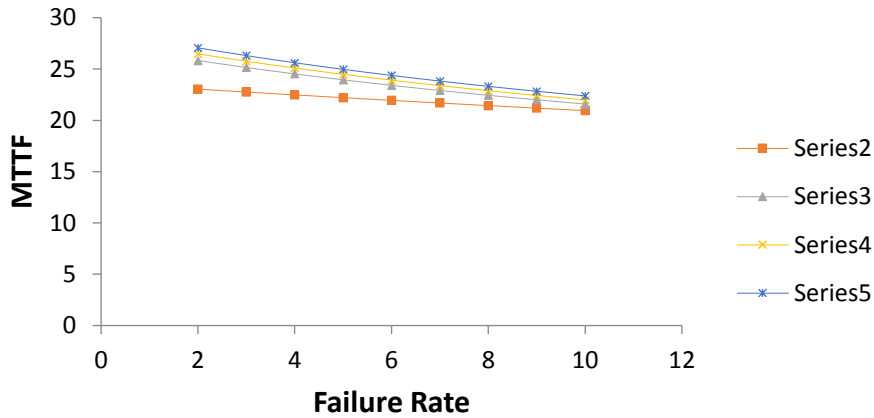


Fig. 6. Impact of rate of failures on MTTF

### 6.5 Sensitivity Analysis

The MTTF sensitivity of the system is calculated by partially differentiating the MTFF with respect to the failure rates of the system. The MTFF sensitivity obtained are shown in Table 6 and the corresponding graph in Table 5

figure 7 by applying the set of parameters as  $v_1 = 0.011$ ,  $v_2 = 0.012$ ,  $v_3 = 0.013$ ,  $v_4 = 0.014$  in the partial differentiation of MTTF.

MTTF sensitivity against the failure rates

Failure rate	$\delta(MTTF)$	$\delta(MTTF)$	$\delta(MTTF)$	$\delta(MTTF)$
	$v_1$	$v_2$	$v_3$	$v_4$
0.001	-285.2646	-703.7950	-750.7016	-789.1233
0.002	-278.8197	-648.6506	-690.2474	-723.6902
0.003	-272.5816	-600.1033	-637.2266	-666.5408
0.004	-266.5417	-557.1427	-590.4689	-616.3337
0.005	-260.6919	-518.9412	-549.0222	-571.9338
0.006	-255.0246	-484.8169	-512.1057	-532.6072
0.007	-249.5324	-454.2040	-479.0755	-497.4785
0.008	-244.2085	-426.6303	-449.3968	-465.9986
0.009	-239.0462	-401.7000	-422.6229	-437.6696

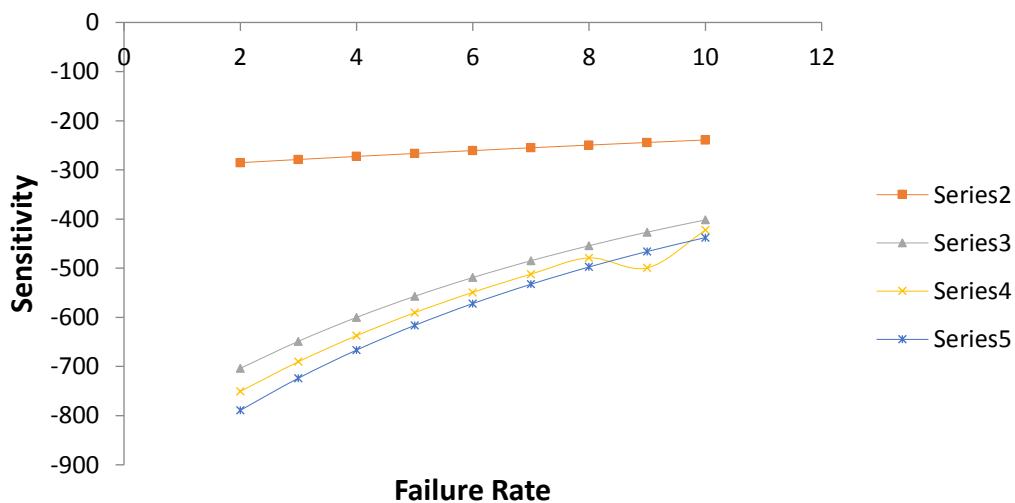


Fig. 7. MTTF sensitivity against failure rate

6.6 Evaluation of Profit when repair follows Copula Distribution

If the service facility is always available, the formula with service facility gives the predicted profit for the interval

$[0, q]$ .  $\kappa_1$  and  $\kappa_2$  service cost per unit time in the interval

$$[0, q] \text{ is } E_p(q) = \kappa_1 \int_0^q R_{up}(q) dq - \kappa_2 q \quad (124)$$

From (118) and (124), the subsequent equation (125) for copula repair follows;

$$E_p(q) = \kappa_1 \left\{ \begin{array}{l} 0.000527e^{-1.01300q} - 0.001753e^{-2.73154q} + 0.012492e^{-1.21995q} + \\ 3.644281e^{-1.11560q} + 3.626311e^{-1.11444q} - 104.117935e^{-0.00975q} + \\ 0.000603e^{-1.01400q} + 0.001293e^{-1.02400q} + 0.001352e^{-1.02800q} + \\ 0.000452e^{-1.01200q} + 0.001327e^{-1.02600q} + 104.101 \end{array} \right\} - \kappa_2 q \quad (125)$$

The anticipated profit for copula repair is calculated using equation (125) as displayed in Table 6 and Figure 8.

Table 6  
 Passage of time with the corresponding profit using copula

$q$	$E_p(q)$ $\kappa_2 = 0.6$	$E_p(q)$ $\kappa_2 = 0.5$	$E_p(q)$ $\kappa_2 = 0.4$	$E_p(q)$ $\kappa_2 = 0.3$	$E_p(q)$ $\kappa_2 = 0.2$	$E_p(q)$ $\kappa_2 = 0.1$
0	0	0	0	0	0	0
1	0.3998	0.4998	0.5998	0.6998	0.7998	0.8998
2	0.7974	0.9974	1.1974	1.3974	1.5974	1.7974
3	1.1878	1.4878	1.7878	2.0878	2.3878	2.6878
4	1.5694	1.9694	2.3694	2.7694	3.1694	3.5694
5	1.9418	2.4418	2.9418	3.4418	3.9418	4.4418
6	2.3048	2.9048	3.5048	4.1048	4.7048	5.3048
7	2.6584	3.3584	4.0584	4.7584	5.4584	6.1584
8	3.0028	3.8028	4.6028	5.4028	6.2028	7.0028
9	3.3381	4.2381	5.1381	6.0381	6.9381	7.8381
10	3.6642	4.6642	5.6642	6.6642	7.6642	8.6642

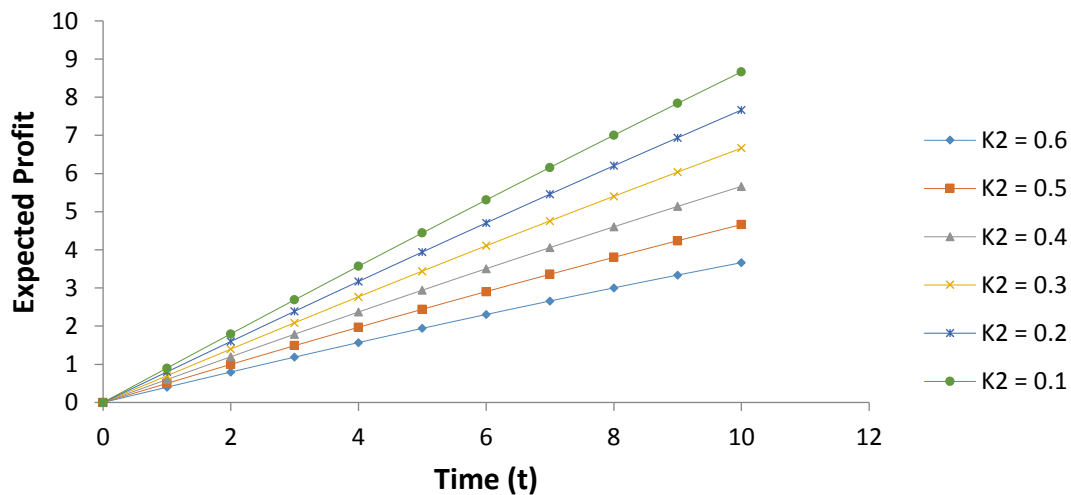


Fig. 8. Time passage with the corresponding profit under copula repair

6.7 Evaluation of Profit when repair follows general repair

The subsequent equation (126) for general repair is as follows;

$$E_p(q) = K_1 \left\{ \begin{aligned} &0.000456e^{-1.01200q} + 0.001339e^{-1.02600q} + 0.001364e^{-0.02800q} + \\ &0.001204e^{-1.02400q} + 0.011384e^{-1.22191q} + 3.108607e^{-1.11560q} + \\ &3.096275e^{-1.11444q} - 48.453700e^{-0.02104q} + 0.000532e^{-1.01300q} \\ &+ 0.000609e^{-1.01400q} + 48.436 \end{aligned} \right\} - K_2q \quad (126)$$

The anticipated profit for general repair is calculated using equation (125) as displayed in Table 7 and Figure 9.

Table 7: Computation of expected profit with respect to time with general repair approach

Table 7  
 Computation of expected profit with respect to time with general repair approach

$q$	$E_p(q)$ $\kappa_2 = 0.6$	$E_p(q)$ $\kappa_2 = 0.5$	$E_p(q)$ $\kappa_2 = 0.4$	$E_p(q)$ $\kappa_2 = 0.3$	$E_p(q)$ $\kappa_2 = 0.2$	$E_p(q)$ $\kappa_2 = 0.1$
0	0	0	0	0	0	0
1	0.3966	0.4966	0.5966	0.6966	0.7966	0.8966
2	0.7809	0.9809	1.1809	1.3809	1.5809	1.7809
3	1.1472	1.4472	1.7472	2.0472	2.3472	2.6472
4	1.4941	1.8941	2.2941	2.6941	3.0941	3.4941
5	1.8215	2.3215	2.8215	3.3215	3.8215	4.3215
6	2.1297	2.7297	3.3297	3.9297	4.5297	5.1297
7	2.4190	3.1190	3.8190	4.5190	5.2190	5.9190
8	2.6897	3.4897	4.2897	5.0897	5.8897	6.6897
9	2.9424	3.8424	4.7424	5.6424	6.5424	7.4424
10	3.1773	4.1773	5.1773	6.1773	7.1773	8.1773

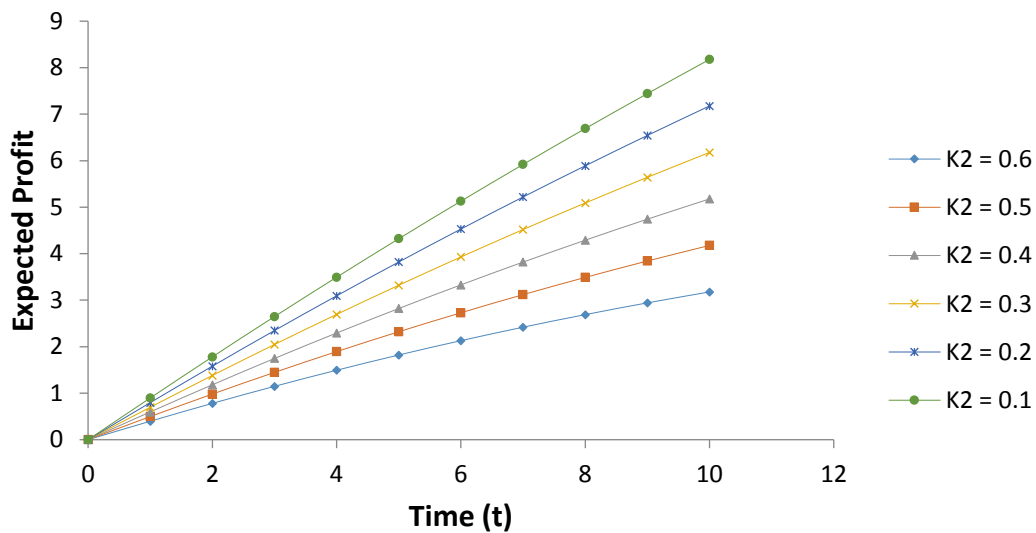


Fig. 9. Time passage with the corresponding profit under general repair

7. Discussion of the Results

Table 1 presents a numerical summary of the system's availability at various time intervals under the copula-based repair policy. The table quantitatively represents the trends illustrated in Figure 2, providing a structured view of how availability evolves over time. The time intervals, presented in distinct rows or columns, could represent

periods such as hours, days, or months. The availability metrics are likely expressed as percentages or fractions, capturing the system's operational performance at specific moments.

Table 2 provides a numerical overview of the system's availability over time when employing general repair strategies. This table serves as a quantitative reference for analyzing the trends depicted in Figure 3, allowing for a

direct comparison with the results obtained using the copula-based repair method. The table likely includes time intervals as rows or columns, reflecting the progression of the system's availability over specific periods such as hours, days, or months. The availability values, expressed as percentages or fractions, capture how the system's operational performance decreases over time.

Comparing these results with those in Table 1 reveals the relative effectiveness of general versus copula-based repair strategies. The data in Table 2 illustrates that the system's availability declines over time under the general repair strategy. While this trend mirrors the decline observed in copula-based strategies, the rate and extent of the decline may differ. The results may suggest that general repair methods are less effective at sustaining high levels of availability over extended periods. Figure 3 offers a graphical representation of the system's availability under general repair strategies, providing a visual counterpart to the numerical trends outlined in Table 2. The X-axis of the graph represents time intervals, while the Y-axis shows system availability as a percentage. The curve in the graph likely shows a downward trend, similar to Figure 2 but potentially steeper or less consistent, depending on the characteristics of the general repair strategy. Together, Table 2 and Figure 3 provide key insights into the system's performance under general repair strategies. They demonstrate that while general repair methods can sustain availability to a degree, their effectiveness diminishes more noticeably over time compared to copula-based approaches. This comparison reinforces the advantages of using specialized repair methods, such as those leveraging copula models, to maintain higher levels of system availability and reliability over extended operational periods.

Figure 4 provides a detailed graphical representation of the system's availability over time, contrasting the performance of copula-based and general repair strategies. The graph uses the X-axis to represent time intervals (e.g., hours, days, or months) and the Y-axis to depict system availability, typically expressed as a percentage. The figure illustrates two distinct curves, each corresponding to one of the repair strategies. The copula-based repair curve shows a relatively stable trend with a less steep decline in availability over the operational period. This indicates that the copula repair strategy effectively mitigates the natural degradation of system performance. The stability of the curve highlights the copula model's ability to capture and manage the complex interdependencies between system components. By addressing these interactions more accurately, the copula approach allows for more efficient maintenance scheduling and resource allocation. This ensures that the system remains operational at higher availability levels for a longer time compared to general repair methods. Conversely, the general repair curve in Figure 4 reveals a more pronounced and rapid decline in system availability as time progresses. This steeper curve suggests that general repair strategies are less effective at preserving system performance. The faster deterioration can be attributed to the general approach's inability to model component interactions as precisely as the copula method. Consequently, maintenance practices under

general repair strategies are less optimized, leading to lower efficiency and a greater loss of availability over time.

Table 3 and Figure 5 provide a graphical representation of system reliability trends over time, complementing the quantitative data presented in Table 3. The figure is titled appropriately to reflect its content, such as "reliability Decline over time for system components." The axes are clearly labeled, with the x-axis representing time and the y-axis representing system reliability, expressed as a probability or percentage. The visualization in Figure 5 likely includes multiple curves or lines, each corresponding to the reliability of individual components or the overall system. These curves illustrate how reliability decreases over time, with some components showing steeper declines due to factors such as high usage rates, design flaws, or material weaknesses. The purpose of Table 3 and Figure 5 is to offer a clear and intuitive understanding of the dynamics of system reliability. It helps identify which components contribute most significantly to the overall reliability decline and highlights the critical times when maintenance or intervention is required. By visually complementing the detailed numerical insights from Table 3, Figure 5 plays a crucial role in identifying patterns, trends, and anomalies, thereby guiding targeted maintenance strategies and design improvements.

Table 4 and Figure 6 provide an in-depth analysis of how varying failure rates ( $v_1$ ,  $v_2$ ,  $v_3$ , and  $v_4$ ) affect the mean time to failure (MTTF) of the respective subsystems, highlighting the relationship between failure rates and system reliability. Table 4 presents detailed numerical data, showing the MTTF for each subsystem under different failure rate scenarios. Each column in the table corresponds to a specific failure rate ( $v_1$ ,  $v_2$ ,  $v_3$ , and  $v_4$ ), with rows listing the associated MTTF values for each subsystem. The data reveals a consistent trend: as failure rates increase, the MTTF decreases. Figure 6 visually complements the data in Table 4, illustrating the decline in MTTF as failure rates increase. The x-axis represents the failure rates ( $v_1$ ,  $v_2$ ,  $v_3$ , and  $v_4$ ), while the y-axis represents the MTTF, measured in appropriate time units. Each subsystem is depicted by a separate curve or line, showing how its MTTF responds to variations in failure rates. The curves indicate differing rates of decline in MTTF among the subsystems, reflecting variations in their robustness against failures. Together, Table 4 and Figure 6 reveal a clear and consistent pattern: as failure rates increase, the MTTF decreases across all subsystems.

The results of profit over time are detailed in Table 6 and Figure 8 for the copula repair strategy and in Table 7 and Figure 9 for the general repair strategy, with a focus on varying service costs  $k_2$  ranging from 0.1 to 0.6. The data from these tables and figures clearly show that, for both repair strategies, profit increases over time regardless of the service cost. This upward trend indicates that as the system operates longer, its profitability grows, reflecting the cumulative benefits of ongoing repairs and maintenance. A closer examination reveals that profit is higher when the service cost  $k_2$  is lower. Specifically, the most significant profits are observed when  $k_2=0.1$  for both

repair strategies. Lower service costs reduce overall expenditure on maintenance and repairs, thereby increasing net profit. This relationship highlights the financial advantage of minimizing service costs while maintaining effective repair practices. Notably, the copula repair strategy consistently generates higher profits compared to the general repair strategy across all service cost levels. This suggests that the copula repair approach is more effective at enhancing profitability, particularly when service costs are reduced. The superior performance of the copula strategy can be attributed to its advanced capability to model dependencies and interactions between system components, leading to more efficient repair and maintenance practices. The analysis demonstrates that the optimal combination for maximizing profit involves both a low service cost  $k_2=0.1$  and the use of the copula repair strategy. This finding underscores the importance of not only minimizing service costs but also optimizing repair strategies to achieve the highest possible profitability. The copula repair strategy, especially when paired with reduced service costs, proves to be the most advantageous approach for maximizing profit, highlighting the critical role of effective cost management and repair optimization in enhancing system profitability. The study's findings offer actionable insights for improving system reliability, managing costs, and enhancing profitability. By adopting the recommended repair strategies and considering the impact of service costs, all stakeholders can contribute to more effective maintenance practices, optimized system performance, and increased overall financial success.

## 8. Conclusion

The study focuses on performance evaluation and reliability modeling in a sequential system that comprises four subsystems. Subsystem 1 has one unit in series with the other subsystems, subsystem 2 has three units in parallel, subsystem 3 has three units in parallel, and subsystem 4 has three units in parallel. The study introduces an innovative methodology by incorporating copula-based repairs, which significantly enhances the system's performance and dependability. The numerical validation of the derived expressions, presented in tables and figures, underscores the advantages of regular copula-based repairs. These repairs are shown to improve the system's reliability and availability, which are crucial for maintaining operational efficiency. The conclusions drawn from the data demonstrate that, generally, the system's profitability, dependability, and availability decline over time. The computed results serve as a valuable tool for decision-makers, allowing them to assess the current state of the system, identify areas for improvement, and make informed decisions to enhance profitability, dependability, and availability. The study provides useful suggestions that can help decision-makers improve system performance, ultimately leading to higher levels of efficiency and productivity across various industries. By offering a detailed understanding of the system's reliability and performance, decision-makers can implement more effective maintenance strategies, such as regular copula-based repairs. This approach can lead to enhanced system performance, higher efficiency, and reduced downtime,

resulting in increased productivity and cost savings for a wide range of industries. The innovative aspects of this study, including the application of copula-based repairs and the comprehensive reliability modeling, contribute significantly to the field, providing new insights and practical solutions for improving centrifugal pump systems. The novelty of this study lies in its comprehensive approach to examining the system's behavior under two different failure scenarios and deriving explicit expressions for critical metrics such as mean time to failure, availability, cost-effectiveness, sensitivity, and reliability. This study provides valuable managerial insights, emphasizing the adoption of copula-based repair methodologies to enhance system reliability, availability, and performance while enabling proactive maintenance strategies to mitigate performance decline over time. It offers a comprehensive framework for performance assessment, allowing managers to identify weak points, prioritize repairs, and allocate resources effectively. The explicit cost-effectiveness analysis aids in aligning maintenance budgets with operational goals, ensuring maximum return on investment. Additionally, the methodology's scalability across industries enables managers in various sectors to improve productivity and efficiency. Finally, the derived metrics, such as mean time to failure and sensitivity analysis, support predictive maintenance strategies and long-term system optimization, fostering sustainability and reducing unexpected failures. This study suggests several directions for future research, including extending the methodology to multi-state systems, exploring the effects of dynamic environmental factors, and optimizing maintenance schedules with predictive analytics. The approach's application to diverse industries and integration with machine learning for real-time failure prediction are also promising avenues. Additionally, detailed economic analyses under varying constraints could enhance its practical relevance. However, the study has limitations, such as its reliance on fixed subsystem configurations and focus on only two failure scenarios, which may limit generalizability. The absence of real-time data and experimental validation reduces practical applicability, while the conclusions drawn from a specific system may require adaptation for broader use. Addressing these gaps will strengthen the methodology's robustness and versatility.

## Conflict of Interest

The authors declared that there is no conflict of interest with regard to this manuscript.

## References

- Abubakar, M.I. and Singh, V.V. (2019) 'Performance assessment of an industrial system (African Textile Manufactures Ltd.) through copula linguistic approach', *Operation Research and Decisions*, Vol. 29, No. 4, pp.1-18.
- Ahmed, S.A., Muiz, A., Mubashir, M and Ahmed, W. (2016). Efficiency enhancement of centrifugal water pump by using in;et guided vanes, *European Journal of Advances in Engineering and Technology*, 3(10), 1-4.
- Bordeasu, D.; Dragan, F.; Filip, I.; Szeidert, I.; Tirian, G.O. Estimation of Centrifugal Pump Efficiency at Variable

- Frequency for Irrigation Systems. *Sustainability* **2024**, 16, 4134. <https://doi.org/10.3390/su16104134>
- Cheng, L.; Zhang, K.-Y.; Zhang, Y.-L.; Jia, X.-Q. Effect on Starting Modes on Centrifugal Pump Performance. *Processes* **2022**, 10, 2362. <https://doi.org/10.3390/pr10112362>
- Dehnavi, E.; Solis, M.; Danlos, A.; Kebdani, M.; Bakir, F. Improving the Performance of an Innovative Centrifugal Pump through the Independent Rotation of an Inducer and Centrifugal Impeller Speeds. *Energies* **2023**, 16, 6321. <https://doi.org/10.3390/en16176321>
- Hawash, S.A., El-gazzar, D.M.S and El-samanoudy, M.A. (2015). Reliability improvements to centrifugal pump performance in conjunction with inducers, CFD comparative study, *Journal of Earth Science and Engineering* 5, 296-305. Doi:10.17265/2159-581X/2015.05.004.
- Jilani, A and Razali, A. (2017). Centrifugal Pump Performance Characteristics for Domestic Application, MATEC Web of Conferences 225, 05011 (2018), UTP-UMP-VIT SES 2018, ) <https://doi.org/10.1051/mateconf/201822505011>
- Jiang, Q., Hen, Y., Liu, X., Zhang, W., Bois, G and Si, Q. (2019). A Review of Design Considerations of Centrifugal Pump Capability for Handling Inlet Gas-Liquid Two-Phase Flows, *Energies*, 12, 1078, 2-18; doi:10.3390/en12061078
- Kumar, A.,Singh, A and Maurya, R.M. (2018). Assessment of Mechanical Problems for Centrifugal Pumps in Eastern Uttar Pradesh, India. *International Journal of Advanced Engineering, Management and Science (IJAEMS)*, 4(9), 686-689.
- Mortazavi, S.M., Mohamadi, M and Jouzdani, J. (2018). MTBF evaluation for 2-out-of-3 redundant repairable systems with common cause and cascade failures considering fuzzy rates for failures and repair: a case study of a centrifugal water pumping system. *Journal of Industrial Engineering International*, 14, 281–291.
- Pagayona, E.; Honra, J. Multi-Criteria Response Surface Optimization of Centrifugal Pump Performance Using CFD for Wastewater Application. *Modelling* **2024**, 5, 673–693. <https://doi.org/10.3390/modelling5030036>
- Poonia, P. (2021) Performance assessment of a multi-state computer network system in series configuration using copula repair. *Int J Reliab Saf* 15(1/2):68–88
- Qazizada, M.E and Pivarciova, E. (2018). Reliability of parallel and serial centrifugal pumps for dewatering in mining process, *Acta Montanistica Slovaca*, 23(2), 141-152.
- Sayed, E., Abdelsamee, A.A and Ghazaly, N.M. (2020). Classification Model using Neural Network for Centrifugal Pump Fault Detection, *International Journal of Systems Signal Control and Engineering Application*, 13(4), 120-126.
- Selvakumar, J and Natarajan, K. (2017). Reliability analysis of centrifugal pump through FMECA and FEM, *International Journal of Performability Engineering*, 13(2), 119-128.
- Singh, V. V., Abubakkar, M. I., Ibrahim, K, H. and Yusuf, I.(2021). Performance assessment of the complex repairable system with n-identical units under (k-out-of-n: G) scheme and copula linguistic repair approach, *Int. J. Q. Reliab. Manage.* **39**(2),367–386
- Singh, V. V., Lado, A. K., Chand, U and Maiti, S. S.(2022). Performance assessment of complex system under the k-out-of-n: G type configuration with k consecutive degraded states through copula repair approach, *Int. J. Q. Reliab. Saf. Eng.* (2022), doi:10.1142/S0218539321500479
- Singh, V.V. and Poonia, P. K. (2022) Stochastic analysis of k-out-of-n: G type of repairable system in combination of subsystems with controllers and multi repair approach. *Journal of Optimization in Industrial Engineering*, Vol. 15, No. 1, pp. 121–130.
- Singh, V.V., Poonia, P.K. and Abdullahi, A.H. (2020). Performance analysis of a complex repairable system with two subsystems in series configuration with an imperfect switch, *J. Math. Comput. Sci.*, 10(2), pp. 359–383.
- Xie, L., Lundteigen, M.A., Liu, Y., Kassa, E and Zhu, S.(2019). Performance Assessment of Safety-instrumented Systems Subject to Cascading Failures in High-demand Mode, Proceedings of the 29th European Safety and Reliability Conference (ESREL),2019, DOI: 10.3850/978-981-11-2724-3\_0318-cd
- Xie, L., Lundteigen, M. A., & Liu, Y. (2021a). Performance assessment of K-out-of-N safety instrumented systems subject to cascading failures. *ISA transactions*, 118, 35-43. <https://doi.org/10.1016/j.isatra.2021.02.015>
- Xie, L., Lundteigen, M. A., & Liu, Y. (2021b). Performance analysis of safety instrumented systems against cascading failures during prolonged demands. *Reliability Engineering & System Safety*, 216, 107975. <https://doi.org/10.1016/j.res.2021.107975>
- Yemane, A and Colledani, M. Performance analysis of unreliable manufacturing systems with uncertain reliability parameters estimated from production data, *International Journal of Computer Integrated Manufacturing*,2019, DOI: 10.1080/0951192X.2019.1644535
- Yuan, Y.; Gong, W.; Wang, G.; Wang, J. Research on the Performance Characteristics and Unsteady Flow Mechanism of a Centrifugal Pump under Pitch Motion. *Water* **2023**, 15, 3706. <https://doi.org/10.3390/w15203706>
- Yusuf, I., Lado, A. I., Singh, V. V., Ali, U. A., & Sufi, N. A. (2020). Performance analysis of multi computer system consisting of three subsystems in series configuration using copula repair policy. *SN Computer Science*, 1, 241. Retrieved from <https://doi.org/10.1007/s>
- Zhu H., Pei J., Wang S., Di J and Huang X. (2019) Reliability Analysis of Centrifugal Pump Based on Small Sample Data. In: Wang K., Wang Y., Strandhagen J., Yu T. (eds) *Advanced Manufacturing and Automation VIII. IWAMA 2018. Lecture Notes in Electrical Engineering*, vol 484. Springer, Singapore. [https://doi.org/10.1007/978-981-13-2375-1\\_17](https://doi.org/10.1007/978-981-13-2375-1_17)
- Zhao,B., Yue, D., Liao, H., Liu, Y and Zhang, X. Performance analysis and optimization of a cold standby system subject to  $\delta$ -shocks and imperfect repairs, *Reliability Engineering and System Safety*,2021, Volume 208. <https://doi.org/10.1016/j.res.2020.107330>

## Appendix Boundary conditions

$$R_1(0, q) = v_1 (R_0(q) + R_2(0, q) + R_3(0, q) + R_4(0, q)) \quad (24)$$

$$R_2(0, q) = 3v_2 R_0(q) \quad (25)$$

$$R_3(0, q) = 3v_3 R_0(q) \tag{26}$$

$$R_4(0, q) = 3v_4 R_0(q) \tag{27}$$

$$R_5(0, q) = 2v_2 R_2(0, q) \tag{28}$$

$$R_6(0, q) = 3v_3 R_2(0, q) \tag{29}$$

$$R_7(0, q) = 3v_4 R_2(0, q) \tag{30}$$

$$R_8(0, q) = v_2 (R_5(0, q) + R_{19}(0, q) + R_{22}(0, q)) \tag{31}$$

$$R_9(0, q) = 3v_2 R_3(0, q) \tag{32}$$

$$R_{10}(0, q) = 2v_3 R_3(0, q) \tag{33}$$

$$R_{11}(0, q) = 3v_4 R_3(0, q) \tag{34}$$

$$R_{12}(0, q) = v_3 (R_{10}(0, q) + R_{17}(0, q) + R_{21}(0, q)) \tag{35}$$

$$R_{13}(0, q) = 3v_2 R_4(0, q) \tag{36}$$

$$R_{14}(0, q) = 3v_3 R_4(0, q) \tag{37}$$

$$R_{15}(0, q) = 2v_4 R_4(0, q) \tag{38}$$

$$R_{16}(0, q) = v_4 (R_{15}(0, q) + R_{18}(0, q) + R_{20}(0, q)) \tag{39}$$

$$R_{17}(0, q) = 2v_3 R_6(0, q) \tag{40}$$

$$R_{18}(0, q) = 2v_4 R_7(0, q) \tag{41}$$

$$R_{19}(0, q) = 2v_2 R_9(0, q) \tag{42}$$

$$R_{20}(0, q) = 2v_4 R_{11}(0, q) \tag{43}$$

$$R_{21}(0, q) = 2v_3 R_{14}(0, q) \tag{44}$$

$$R_{22}(0, q) = 2v_2 R_{13}(0, q) \tag{45}$$

With initial condition

$$R_k(0) = \begin{cases} 1, & k = 0 \\ 0, & \text{otherwise} \end{cases} \tag{46}$$

Taking Laplace transformation of equations (1) – (23) and using (46), to obtain the following:

$$(s + v_1 + 3v_2 + 3v_3 + 3v_4) \bar{R}_0(q) = 1 + \int_0^\infty \beta_0(e_2) R_2(e_2, s) de_2 + \int_0^\infty \beta_0(e_4) \bar{R}_3(e_3, s) de_3 + \int_0^\infty \beta_0(e_4) \bar{R}_4(e_4, s) de_4 + \int_0^\infty h_0(e_1) \bar{R}_1(e_1, s) de_1 + \int_0^\infty h_0(e_2) \bar{R}_8(e_2, s) de_2 + \int_0^\infty h_0(e_3) \bar{R}_{12}(e_3, s) de_3 + \int_0^\infty h_0(e_4) \bar{R}_{16}(e_4, s) de_4 \quad (47)$$

$$\left( s + \frac{\delta}{\delta e_1} + h_0(e_1) \right) \bar{R}_1(e_1, s) = 0 \quad (48)$$

$$\left( s + \frac{\delta}{\delta e_2} + v_1 + 2v_2 + 3v_3 + 3v_4 + \beta_0(e_2) \right) \bar{R}_2(e_2, s) = 0 \quad (49)$$

$$\left( s + \frac{\delta}{\delta e_3} + v_1 + 3v_2 + 2v_3 + 3v_4 + \beta_0(e_3) \right) \bar{R}_3(e_3, s) = 0 \quad (50)$$

$$\left( s + \frac{\delta}{\delta e_4} + v_1 + 3v_2 + 3v_3 + 2v_4 + \beta_0(e_4) \right) \bar{R}_4(e_4, s) = 0 \quad (51)$$

$$\left( s + \frac{\delta}{\delta e_2} + v_2 + \beta_0(e_2) \right) \bar{R}_5(e_2, s) = 0 \quad (52)$$

$$\left( s + \frac{\delta}{\delta e_3} + 2v_3 + \beta_0(e_3) \right) \bar{R}_6(e_3, s) = 0 \quad (53)$$

$$\left( s + \frac{\delta}{\delta e_4} + 2v_4 + \beta_0(e_4) \right) \bar{R}_7(e_4, s) = 0 \quad (54)$$

$$\left( s + \frac{\delta}{\delta e_2} + h_0(e_2) \right) \bar{R}_8(e_2, s) = 0 \quad (55)$$

$$\left( s + \frac{\delta}{\delta e_2} + 2v_2 + \beta_0(e_2) \right) \bar{R}_9(e_2, s) = 0 \quad (56)$$

$$\left( s + \frac{\delta}{\delta e_3} + v_3 + \beta_0(e_3) \right) \bar{R}_{10}(e_3, s) = 0 \quad (57)$$

$$\left( s + \frac{\delta}{\delta e_4} + 2v_4 + \beta_0(e_4) \right) \bar{R}_{11}(e_4, s) = 0 \quad (58)$$

$$\left( s + \frac{\delta}{\delta e_3} + h_0(e_3) \right) \bar{R}_{12}(e_3, s) = 0 \quad (59)$$

$$\left( s + \frac{\delta}{\delta e_2} + 2v_2 + \beta_0(e_2) \right) \bar{R}_{13}(e_2, s) = 0 \quad (60)$$

$$\left( s + \frac{\delta}{\delta e_3} + 2v_3 + \beta_0(e_3) \right) \bar{R}_{14}(e_3, s) = 0 \quad (61)$$

$$\left( s + \frac{\delta}{\delta e_4} + v_4 + \beta_0(e_4) \right) \overline{R}_{15}(e_4, s) = 0 \quad (62)$$

$$\left( s + \frac{\delta}{\delta e_4} + h_0(e_4) \right) \overline{R}_{16}(e_4, s) = 0 \quad (63)$$

$$\left( s + \frac{\delta}{\delta e_3} + v_3 + \beta_0(e_3) \right) \overline{R}_{17}(e_3, s) = 0 \quad (64)$$

$$\left( s + \frac{\delta}{\delta e_4} + v_4 + \beta_0(e_4) \right) \overline{R}_{18}(e_4, s) = 0 \quad (65)$$

$$\left( s + \frac{\delta}{\delta e_2} + v_2 + \beta_0(e_2) \right) \overline{R}_{19}(e_2, s) = 0 \quad (66)$$

$$\left( s + \frac{\delta}{\delta e_4} + v_4 + \beta_0(e_4) \right) \overline{R}_{20}(e_4, s) = 0 \quad (67)$$

$$\left( s + \frac{\delta}{\delta e_3} + v_3 + \beta_0(e_3) \right) \overline{R}_{21}(e_3, s) = 0 \quad (68)$$

$$\left( s + \frac{\delta}{\delta e_2} + v_2 + \beta_0(e_2) \right) \overline{R}_{22}(e_2, s) = 0 \quad (69)$$

Laplace transform of boundary conditions

$$\overline{R}_1(0, s) = v_1 \left[ \overline{R}_0(s) + \overline{R}_2(0, s) + \overline{R}_3(0, s) + \overline{R}_4(0, s) \right] \quad (70)$$

$$\overline{R}_2(0, s) = 3v_2 \overline{R}_0(s) \quad (71)$$

$$\overline{R}_3(0, s) = 3v_3 \overline{R}_0(s) \quad (72)$$

$$\overline{R}_4(0, s) = 3v_4 \overline{R}_0(s) \quad (73)$$

$$\overline{R}_5(0, s) = 2v_2 \overline{R}_2(0, s) \quad (74)$$

$$\overline{R}_6(0, s) = 3v_3 \overline{R}_2(0, s) \quad (75)$$

$$\overline{R}_7(0, s) = 3v_4 \overline{R}_2(0, s) \quad (76)$$

$$\overline{R}_8(0, s) = v_2 \left[ \overline{R}_5(0, s) + \overline{R}_{19}(0, s) + \overline{R}_{22}(0, s) \right] \quad (77)$$

$$\overline{R}_9(0, s) = 3v_2 \overline{R}_3(0, s) \quad (78)$$

$$\overline{R}_{10}(0, s) = 2v_3 \overline{R}_3(0, s) \quad (79)$$

$$\overline{R}_{11}(0, s) = 3v_4 \overline{R}_3(0, s) \quad (80)$$

$$\overline{R}_{12}(0, s) = v_3 \left[ \overline{R}_{10}(0, s) + \overline{R}_{17}(0, s) + \overline{R}_{21}(0, s) \right] \quad (81)$$

$$\bar{R}_{13}(0, s) = 3v_2 \bar{R}_4(0, s) \quad (82)$$

$$\bar{R}_{14}(0, s) = 3v_3 \bar{R}_4(0, s) \quad (83)$$

$$\bar{R}_{15}(0, s) = 2v_4 \bar{R}_4(0, s) \quad (84)$$

$$\bar{R}_{16}(0, s) = v_4 \left[ \bar{R}_{15}(0, s) + \bar{R}_{20}(0, s) + \bar{R}_{18}(0, s) \right] \quad (85)$$

$$\bar{R}_{17}(0, s) = 2v_4 \bar{R}_6(0, s) \quad (86)$$

$$\bar{R}_{18}(0, s) = 2v_4 \bar{R}_7(0, s) \quad (87)$$

$$\bar{R}_{19}(0, s) = 2v_2 \bar{R}_9(0, s) \quad (88)$$

$$\bar{R}_{20}(0, s) = 2v_4 \bar{R}_{11}(0, s) \quad (89)$$

$$\bar{R}_{21}(0, s) = 2v_3 \bar{R}_{14}(0, s) \quad (90)$$

$$\bar{R}_{22}(0, s) = 2v_2 \bar{R}_{13}(0, s) \quad (91)$$

Solving (47)–(69), using (70)–(91) to obtained

$$\bar{R}_0(s) = \frac{1}{D(s)} \quad (92)$$

$$\bar{R}_1(s) = \left( \frac{(v_1 + 3v_1v_2 + 3v_1v_3 + 3v_1v_4)(1 - \bar{S}_\mu(s))}{sD(s)} \right) \quad (93)$$

$$\bar{R}_2(s) = \frac{3v_2(1 - \bar{S}_\phi(s + v_1 + 2v_2 + 3v_3 + 3v_4))}{(s + v_1 + 2v_2 + 3v_3 + 3v_4)D(s)} \quad (94)$$

$$\bar{R}_3(s) = \frac{3v_3(1 - \bar{S}_\phi(s + v_1 + 3v_2 + 2v_3 + 3v_4))}{(s + v_1 + 3v_2 + 2v_3 + 3v_4)D(s)} \quad (95)$$

$$\bar{R}_4(s) = \frac{3v_4(1 - \bar{S}_\phi(s + v_1 + 3v_2 + 3v_3 + 2v_4))}{(s + v_1 + 3v_2 + 3v_3 + 2v_4)D(s)} \quad (96)$$

$$\bar{R}_5(s) = \frac{6v_2^2(1 - \bar{S}_\phi(s + v_2))}{(s + v_2)D(s)} \quad (97)$$

$$\bar{R}_6(s) = \frac{9v_2v_3(1 - \bar{S}_\phi(s + 2v_3))}{(s + 2v_3)D(s)} \quad (98)$$

$$\bar{R}_7(s) = \frac{9v_2v_4(1 - \bar{S}_\phi(s + 2v_4))}{(s + 2v_4)D(s)} \quad (99)$$

$$\bar{R}_8(s) = \frac{(6v_2^3 + 18v_2^3v_3 + 18v_2^3v_4)(1 - \bar{S}_\mu(s))}{sD(s)} \quad (100)$$

$$\bar{R}_9(s) = \frac{9v_2v_3(1 - \bar{S}_\phi(s + 2v_2))}{(s + 2v_2)D(s)} \quad (101)$$

$$\bar{R}_{10}(s) = \frac{6v_3^2(1 - \bar{S}_\phi(s + v_3))}{(s + v_3)D(s)} \quad (102)$$

$$\bar{R}_{11}(s) = \frac{9v_3v_4(1 - \bar{S}_\phi(s + 2v_4))}{(s + 2v_4)D(s)} \quad (103)$$

$$\bar{R}_{12}(s) = \frac{(6v_3^3 + 18v_2v_3^2v_4 + 18v_3^3v_4)(1 - \bar{S}_\mu(s))}{sD(s)} \quad (104)$$

$$\bar{R}_{13}(s) = \frac{9v_2v_4(1 - \bar{S}_\phi(s + 2v_2))}{(s + 2v_2)D(s)} \quad (105)$$

$$\bar{R}_{14}(s) = \frac{9v_3v_4(1 - \bar{S}_\phi(s + 2v_3))}{(s + 2v_3)D(s)} \quad (106)$$

$$\bar{R}_{15}(s) = \frac{6v_4^2(1 - \bar{S}_\phi(s + v_4))}{(s + v_4)D(s)} \quad (107)$$

$$\bar{R}_{16}(s) = \frac{(6v_4^3 + 18v_4^3v_3 + 18v_4^3v_2)(1 - \bar{S}_\mu(s))}{sD(s)} \quad (108)$$

$$\bar{R}_{17}(s) = \frac{18v_2v_3v_4(1 - \bar{S}_\phi(s + v_3))}{(s + v_3)D(s)} \quad (109)$$

$$\bar{R}_{18}(s) = \frac{18v_2v_4^2(1 - \bar{S}_\phi(s + v_4))}{(s + v_4)D(s)} \quad (110)$$

$$\bar{R}_{19}(s) = \frac{18v_2^2v_3(1 - \bar{S}_\phi(s + v_2))}{(s + v_2)D(s)} \quad (111)$$

$$\bar{R}_{20}(s) = \frac{18v_4^2v_3(1 - \bar{S}_\phi(s + v_4))}{(s + v_4)D(s)} \quad (113)$$

$$\bar{R}_{21}(s) = \frac{18v_3^2v_4(1 - \bar{S}_\phi(s + v_3))}{(s + v_3)D(s)} \quad (114)$$

$$\bar{R}_{22}(s) = \frac{18v_2^2v_4(1 - \bar{S}_\phi(s + v_2))}{(s + v_2)D(s)} \quad (115)$$

Where

$$D(s) = \left\{ \begin{aligned} & s + v_1 + 3v_2 + 3v_3 + 3v_4 - \{3v_2\bar{S}_\phi(s + v_1 + 2v_2 + 3v_3 + 3v_4)\bar{S}_\mu(s) \\ & + 3v_3\bar{S}_\phi(s + v_1 + 3v_2 + 2v_3 + 3v_4) + 3v_4\bar{S}_\phi(s + v_1 + 3v_2 + 3v_3 + 2v_4)\bar{S}_\mu(s) \} \\ & + (v_1 + 3v_1v_2 + 3v_1v_3 + 3v_1v_4)\bar{S}_\mu(s) + (6v_2^3 + 18v_2^2v_3 + 18v_2^2v_4)\bar{S}_\mu(s) \\ & + (6v_3^3 + 18v_2v_3^2v_4 + 18v_3^2v_4)\bar{S}_\mu(s) + (6v_4^3 + 18v_2v_4^2v_3 + 18v_4^2v_3^2)\bar{S}_\mu(s) \} \end{aligned} \right. \quad (116)$$

and

$$\bar{R}_{up}(s) = \frac{1}{D(s)} \left\{ \begin{aligned} & \bar{R}_0(s) + \bar{R}_2(s) + \bar{R}_3(s) + \bar{R}_4(s) + \bar{R}_5(s) + \bar{R}_6(s) + \bar{R}_7(s) \\ & + \bar{R}_9(s) + \bar{R}_{10}(s) + \bar{R}_{11}(s) + \bar{R}_{13}(s) + \bar{R}_{14}(s) + \bar{R}_{15}(s) + \bar{R}_{17}(s) \\ & + \bar{R}_{18}(s) + \bar{R}_{19}(s) + \bar{R}_{20}(s) + \bar{R}_{21}(s) + \bar{R}_{22}(s) \end{aligned} \right. \quad (117)$$

$$\bar{R}_{up}(s) = \frac{1}{D(s)} \left\{ \begin{aligned} & 1 + \frac{3v_2(1 - \bar{S}_\phi(s + v_1 + 2v_2 + 3v_3 + 3v_4))}{(s + v_1 + 2v_2 + 3v_3 + 3v_4)} + \frac{3v_3(1 - \bar{S}_\phi(s + v_1 + 3v_2 + 2v_3 + 3v_4))}{(s + v_1 + 3v_2 + 2v_3 + 3v_4)} + \\ & \frac{3v_4(1 - \bar{S}_\phi(s + v_1 + 3v_2 + 3v_3 + 2v_4))}{(s + v_1 + 3v_2 + 3v_3 + 2v_4)} + \frac{6v_2^2(1 - \bar{S}_\phi(s + v_2))}{(s + v_2)} + \frac{9v_2v_3(1 - \bar{S}_\phi(s + 2v_3))}{(s + 2v_3)} + \\ & \frac{9v_2v_4(1 - \bar{S}_\phi(s + 2v_4))}{(s + 2v_4)} + \frac{9v_2v_3(1 - \bar{S}_\phi(s + 2v_2))}{(s + 2v_2)} + \frac{6v_3^2(1 - \bar{S}_\phi(s + v_3))}{(s + v_3)} \\ & + \frac{9v_3v_4(1 - \bar{S}_\phi(s + 2v_4))}{(s + 2v_4)} + \frac{9v_2v_4(1 - \bar{S}_\phi(s + 2v_2))}{(s + 2v_2)} + \frac{9v_3v_4(1 - \bar{S}_\phi(s + 2v_3))}{(s + 2v_3)} + \\ & \frac{6v_4^2(1 - \bar{S}_\phi(s + v_4))}{(s + v_4)} + \frac{18v_2v_3v_4(1 - \bar{S}_\phi(s + v_3))}{(s + v_3)} + \frac{18v_2v_4^2(1 - \bar{S}_\phi(s + v_4))}{(l_0 + \lambda_4)} + \\ & \frac{18v_2^2v_3(1 - \bar{S}_\phi(s + v_2))}{(s + v_2)} + \frac{18v_4^2v_3(1 - \bar{S}_\phi(s + v_4))}{(s + v_4)} + \frac{18v_3^2v_4(1 - \bar{S}_\phi(s + v_3))}{(s + v_3)} \\ & + \frac{18v_2^2v_4(1 - \bar{S}_\phi(s + v_2))}{(s + v_2)} \end{aligned} \right. \quad (118)$$

$$\bar{R}_{down}(s) = 1 - \bar{R}_{up}(s) \quad (119)$$